BNL-75681-2006-JA

Atmos. Chem. Phys., 6, 4723–4738, 2006
www.atmos-chem-phys.net/6/4723/2006/

Atmospheric Chemistry and Physics

Attribution of modeled atmospheric sulfate and SO_2 in the Northern Hemisphere for June–July 1997

C. M. Benkovitz, S. E. Schwartz, M. P. Jensen, and M. A. Miller

Brookhaven National Laboratory, P.O. Box 5000, Upton, NY 11973, USA

Received: 16 January 2006 – Published in Atmos. Chem. Phys. Discuss.: 22 May 2006
Revised: 1 August 2006 – Accepted: 15 October 2006 – Published: 23 October 2006

Abstract. Anthropogenic sulfate aerosol is a major contributor to shortwave radiative forcing of climate change by direct light scattering and by perturbing cloud properties and to local concentrations of atmospheric particulate matter. Here we analyze results from previously published calculations with an Eulerian transport model for atmospheric sulfur species in the Northern Hemisphere in June–July, 1997 to quantify the absolute and relative contributions of specific source regions (North America, Europe, and Asia) and SO_2-to-sulfate conversion mechanisms (gas-phase, aqueous-phase and primary sulfate) to sulfate and SO_2 column burdens as a function of location and time. Although material emitted within a given region dominates the sulfate and SO_2 column burden in that region, examination of time series at specific locations shows that material imported from outside can make a substantial and occasionally dominant contribution. Frequently the major fraction of these exogenous contributions to the sulfate column burden was present aloft, thus minimally impacting air quality at the surface, but contributing substantially to the burden and, by implication, to radiative forcing and diminution of surface irradiance. Although the dominant sulfate formation pathway in the domain as a whole is aqueous-phase reaction in clouds (62%), in regions with minimum opportunity for aqueous-phase reaction gas-phase oxidation is dominant, albeit with considerable temporal variability depending on meteorological conditions. These calculations highlight the importance of transoceanic transport of sulfate, especially at the western margins of continents under the influence of predominantly westerly transport winds.

Correspondence to: C. M. Benkovitz
(cmb@bnl.gov)

1 Introduction

Anthropogenic aerosols are thought to be influencing climate by offsetting the radiative forcing of greenhouse gases (Penner et al., 2001; Ramaswamy et al., 2001; Bellouin et al., 2005) via scattering and absorption of radiation (direct effect) and by enhancing the reflectivity and lifetimes of clouds (indirect effect). Aerosol forcing is strongest in the industrialized areas of North America, Europe, and Asia (Ramaswamy et al., 2001). Solar radiation reaching the surface of the Earth has decreased discernibly during the past 50 years (Liepert, 2002; Stanhill and Cohen, 2001); these decreases also are more pronounced in industrialized areas. Atmospheric aerosols also contribute to deterioration of air quality in industrialized areas affecting human health and welfare. A major component of aerosols in these areas is sulfate resulting from the atmospheric oxidation of anthropogenically emitted sulfur dioxide (SO_2) (U.S. Environmental Protection Agency, 2001). The long-range transport of anthropogenic sulfate aerosols (Perry et al., 1999; Piketh et al., 2002) suggests the need for quantifying the extent of the influence of source regions and source types on sulfate and SO_2 mixing ratios and column burdens.

A variety of approaches have been used to determine the influence of source regions and source types on the burdens of atmospheric trace species. Simulations using Eulerian models have been performed with and without emissions from certain source regions (Yienger et al., 2000); the influence of those source regions is estimated as the difference in the atmospheric burden between the two simulations. This method is suitable provided removing the selected sources does not appreciably alter the chemistry of the species being studied, but for species such as sulfur and nitrogen whose chemistry alters atmospheric concentrations of oxidant species this method may result in approximate estimates only. Lagrangian models that track emitted parcels individually have been used to model regional transport (Mal-

Published by Copernicus GmbH on behalf of the European Geosciences Union.

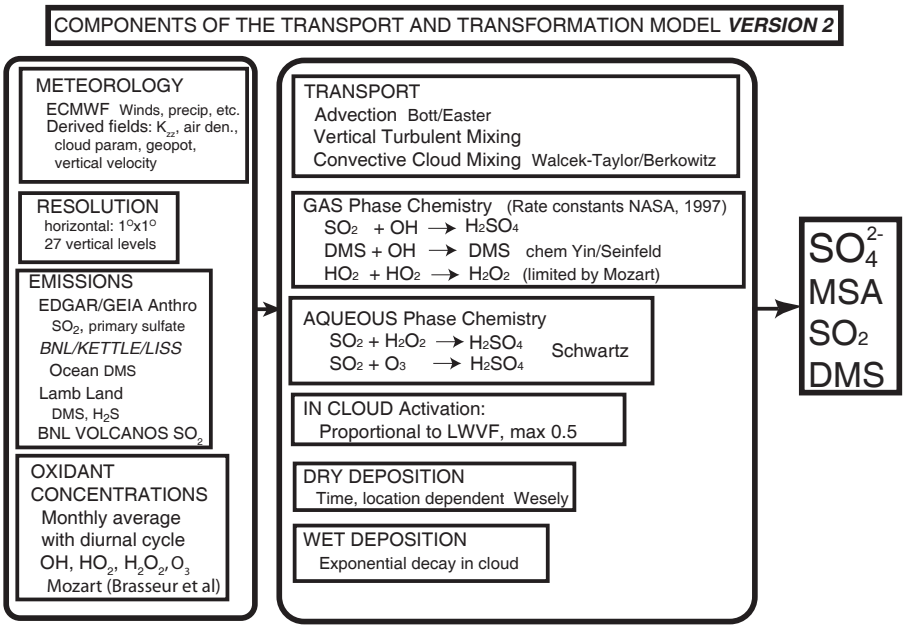

Fig. 1. Schematic of the processes included in the Global Chemistry Model driven by observation-derived meteorology (GChM-O). Here, BNL/Kettle/Liss, Brookhaven National Laboratory, Kettle et al. (1999), Liss and Merlivat (1986); Lamb (Bates et al., 1992); Horowitz (2003); Bott/Easter (Bott, 1989; Easter, 1993); Easter and Luecken (1988); Walcek-Taylor/Berkowitz (Walcek and Taylor, 1986); NASA (1997); Yin/Seinfeld (Yin et al., 1990a, b); Schwartz (1988); Wesely (Sheih et al., 1986; Wesely, 1989), and Benkovitz et al. (1994).

com et al., 2000). Concerns with this approach include representation of the interactions among species from multiple sources. Measurements coupled with air-mass back trajectory calculations have been used to determine potential source regions of the measured species (Jaffe et al., 1999; Martin et al., 2003; Perry et al., 1999; Allan et al., 2004). For example, Allan et al. (2004) presented an instance at Trinidad Head, California, in which appreciable non-seasalt sulfate was present in an airmass directly from the west that had had no discernible influence from North American sources. However this method is limited to the times and locations where measurements have been performed, and uncertainties and limitations in the back trajectory analyses grow quickly with time and may identify different source regions depending on the type of back trajectory analysis performed. With varying degrees of uncertainty all these methods are able to qualitatively represent the influences of various source regions on the amount of material at receptor locations of interest; however, quantification of these influences is rarely possible and subject to large uncertainties.

Eulerian models with accurate representations of the sulfur cycle and the ability to track sulfur by source regions and source types are capable of more rigorous quantitative studies (Benkovitz et al., 1994; Graf et al., 1997; Rasch et al., 2000; Uno et al., 2003). Benkovitz et al. (1994) used an Eulerian sub-hemispheric chemical transport model with emissions labeled by source type (anthropogenic, biogenic) and source region (North America and Europe) to study the sulfate and SO_2 burdens for four seasonal six-week periods in 1986–1987. Sulfate concentrations and column burdens exhibited rich temporal and spatial structure related to existing meteorological patterns for each season. For the October-November 1986 simulation a pronounced variability was found in the contribution of the source regions to the sulfate burden over oceanic areas; over the mid north Atlantic the variation over a six-hour period in the fraction of the burden due to North American sources was between 25 and 58% and the variation in the fraction due to European sources was between 2 and 33%. Graf et al. (1997) carried out a five-year simulation with the Hamburg climate model European Centre Hamburg (ECHAM) global general circulation model (GCM) with a representation of the sulfur cycle to estimate the contribution of volcanic emissions to the global sulfur distribution. Material was attributed to specific sources (anthropogenic, biomass burning, DMS and volcanic) by determining the ratio of the contribution of the various sources to the total sulfur budget and treating emissions from these sources as separate variables. Although the global annual contributions of anthropogenic sulfur emissions exceeded that of volcanic emissions by a factor of $\sim$5, the fractional contributions of the two sources to the total sulfate budget were found to be similar. However, strong interhemispheric and seasonal differences were found in the relative contributions of the various sulfur sources. Uno et al. (2003) integrated a chemical transport model within the Regional Atmospheric Modeling System (Pielke et al., 1992), which in-

cluded anthropogenic sulfur, dust, black carbon, organic carbon, CO from anthropogenic sources and from biomass burning, sea salt, lightning NO_x, volcanic SO_2, and radon. The influence of volcanic SO_2 was mimicked using an unreactive tracer, which allowed qualitative knowledge of which air masses were affected by these emissions. The sulfur chemistry was represented online as a simplified 1% h^{-1} conversion rate; photochemical processes were calculated offline using other models. This model was applied to the east Asia and western Pacific region and used for forecast and post-experiment analyses during the ACE-Asia field experiment. Rasch et al. (2000) used a global GCM with a representation of the sulfur cycle to perform a three-year simulation in which sulfur emissions were identified by region of origin (North America, Europe, Asia, rest of the world) and source type (anthropogenic, biogenic). Substantial differences were found in the turnover time (mean residence time), sulfate potential (defined as the ratio of the sulfate burden to the SO_2 emissions), and contribution to the sulfate burden for the several source regions. For example, North American sources were the principal contributors to the annual averaged sulfate column burden over the North Atlantic; Asian sources contributed over 50% of the burden over the north Pacific Ocean to the west coast of North America, and also contributed up to ~40% of the burden in the southern hemisphere.

In the work described here a three-dimensional hemispheric Eulerian chemical transport model for sulfur was used to simulate the June–July 1997 time period for the Northern Hemisphere from the equator to 81° N and to examine the influence of source regions and source types on the sulfate and SO_2 burdens. A six-week simulation was performed; the first two weeks were considered model spinup time and results were not analyzed. The model used in this study, the Global Chemistry Model driven by Observation-derived meteorological data (GChM-O), a three-dimensional Eulerian transport and transformation model for sulfate, methanesulfonic acid (MSA), and precursor species has previously been described and extensively evaluated by comparison with observations (Benkovitz et al., 2004). A brief description of the model is presented in Appendix A, a schematic is presented in Fig. 1, and the geographical distribution of sulfur emissions is presented in Fig. 2.

The model has been extensively compared with observations using mostly 24-h sulfate and SO_2 mixing ratios (Benkovitz et al., 2004, 2003). For sulfate in ~5000 evaluation points 50% of the modeled 24-h mixing ratios were within a factor of 1.85 of the observations; for SO_2 in ~12 600 evaluation points 50% of the modeled 24-h mixing ratios were within a factor of 2.55 of the observations. These results indicate that a fraction of model observation differences was due to subgrid variation and/or measurement with the balance of the difference attributed to model error. Examination of key diagnostic quantities calculated from model results showed substantial variation for the different source regions and source types, e.g., SO_2 aqueous-phase oxidation rates of 29 to 102% day^{-1}, SO_2 dry deposition rates of 3 to 32% day^{-1}, sulfate residence times of 4 to 9 days. These differences were attributed to differences in the relative mixing ratios of SO_2 and H_2O_2 and to the fraction of SO_2 and sulfate in clouds for the various source regions and source types.

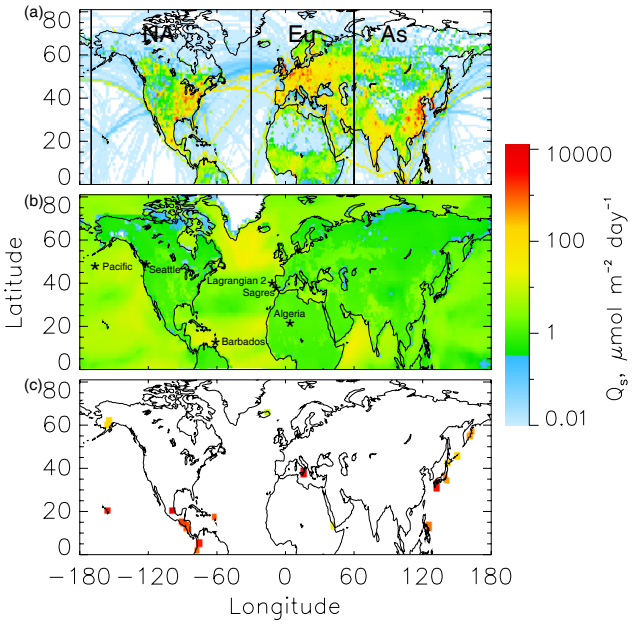

Fig. 2. Sulfur emissions for the simulation period: **(a)** anthropogenic sources, **(b)** average biogenic sources, **(c)** average volcanic sources. All panels use the scale shown. Volcanic emissions were divided by the area of the model grid cell where the volcano is located and the surrounding grid cells have been given the same color key to increase the visibility of the location of each volcano. The north-south lines in (a) delimit the anthropogenic source regions distinguished in the model, North America (NA), Europe (Eu), Asia (As). Locations marked in panel (b) are those at which detailed source attribution was conducted for sulfate and SO_2 (Sect. 4).

2 Attribution of sulfate and SO_2 burdens

The geographic extent of the influence of individual source regions and source types is first examined using the average fractional contribution to the total sulfate column burden (Fig. 3) and to the total SO_2 column burden (Fig. 4) for the entire simulation period; the column burden, the vertical integral of the concentration, is the pertinent quantity affecting aerosol light scattering and extinction. The average fractional contribution F_r of material emitted in source region r at a location of interest for a time period extending over multiple model time periods is calculated as:

$$\overline{F_r} = \frac{\sum_t B_{r,t}}{\sum_t B_{\mathrm{tot},t}} \quad (1)$$

where $B_{r,t}$ is the column burden at that location derived from emissions in source region r at model time period t and $B_{\mathrm{tot},t}$

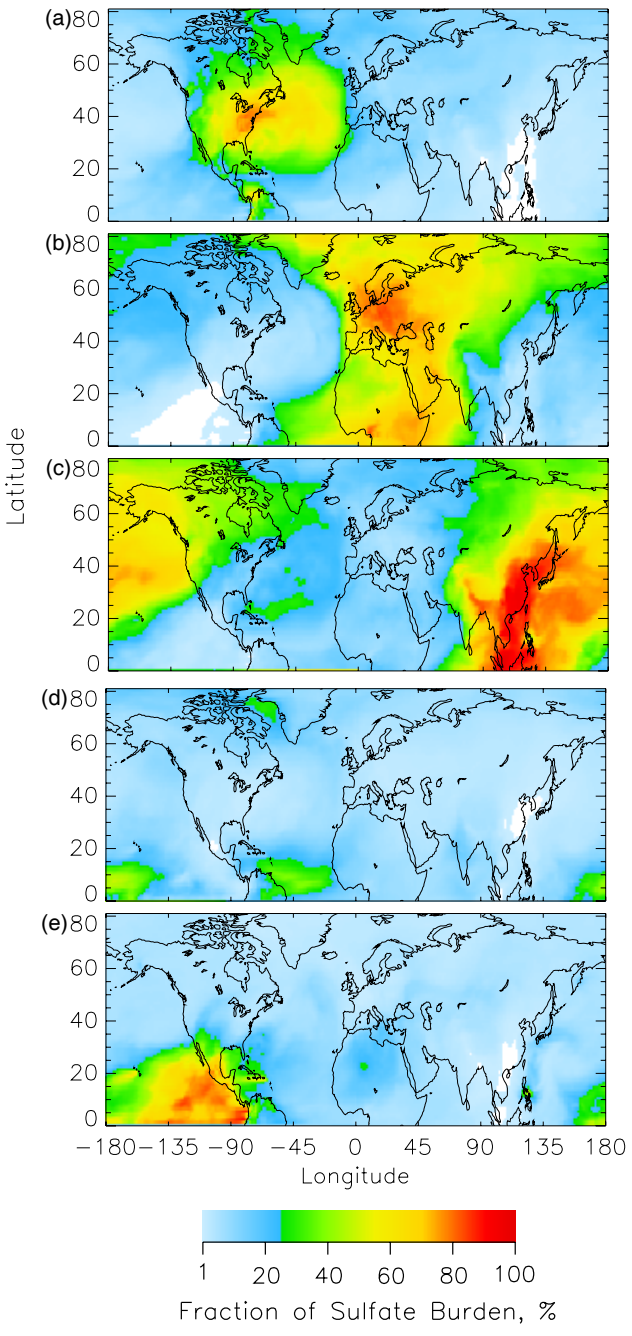

Fig. 3. Average fraction (%) of the different source regions and source types to the sulfate column burden for the 6-week analysis period as a function of location in the model domain. **(a)** North American sources, **(b)** European sources, **(c)** Asian sources, **(d)** biogenic sources, and **(e)** volcanic sources. White indicates areas where contribution was less than 1%.

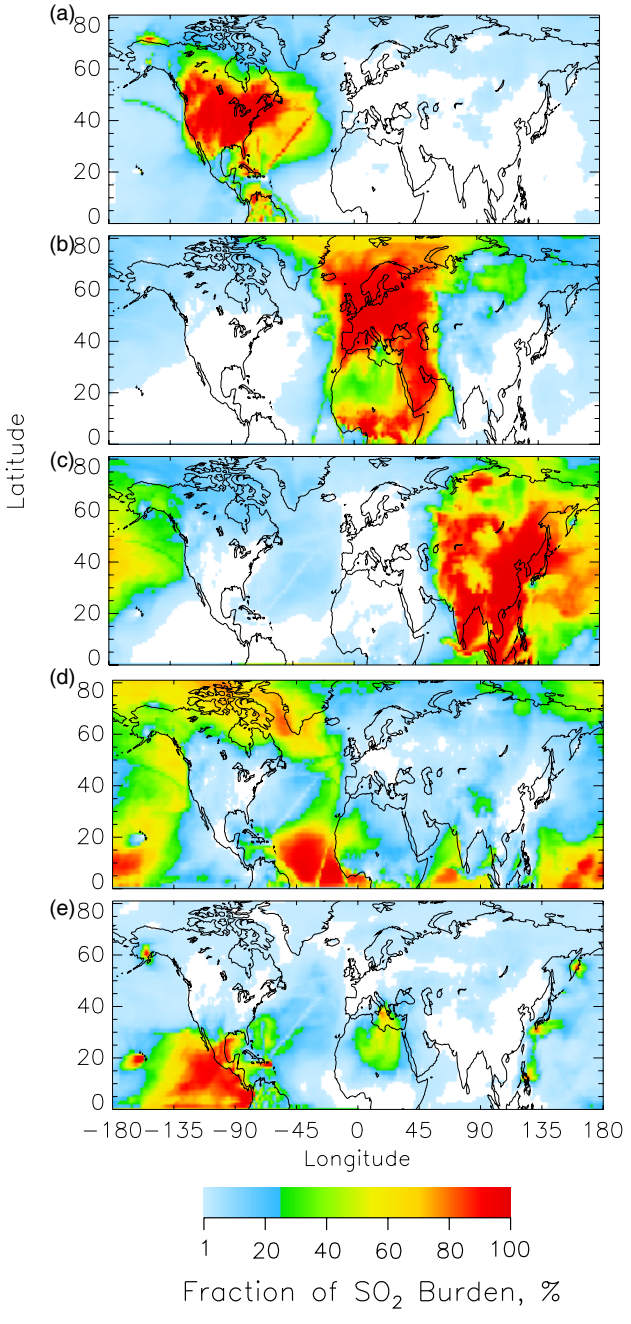

Fig. 4. Average fractional contribution (%) of source regions and source types to the total SO_2 column burden for the 6-week analysis period, **(a)** North American sources, **(b)** European sources, **(c)** Asian sources, **(d)** biogenic sources, and **(e)** volcanic sources. White indicates areas where contribution was less than 1%.

is the total column burden at that location at model time period t; fractional contribution of a source region to mixing ratio is evaluated similarly. As expected, each of the three major anthropogenic source regions (North America, NA; Europe, Eu; and Asia, As) was the principal contributor to the column burdens in its own region, reflective of the relatively short turnover time (∼7 days) for sulfate and the much shorter turnover time (∼1 day) for SO_2 (Benkovitz et al., 2004) as compared to the time needed for material to become distributed over the entire Northern Hemisphere.

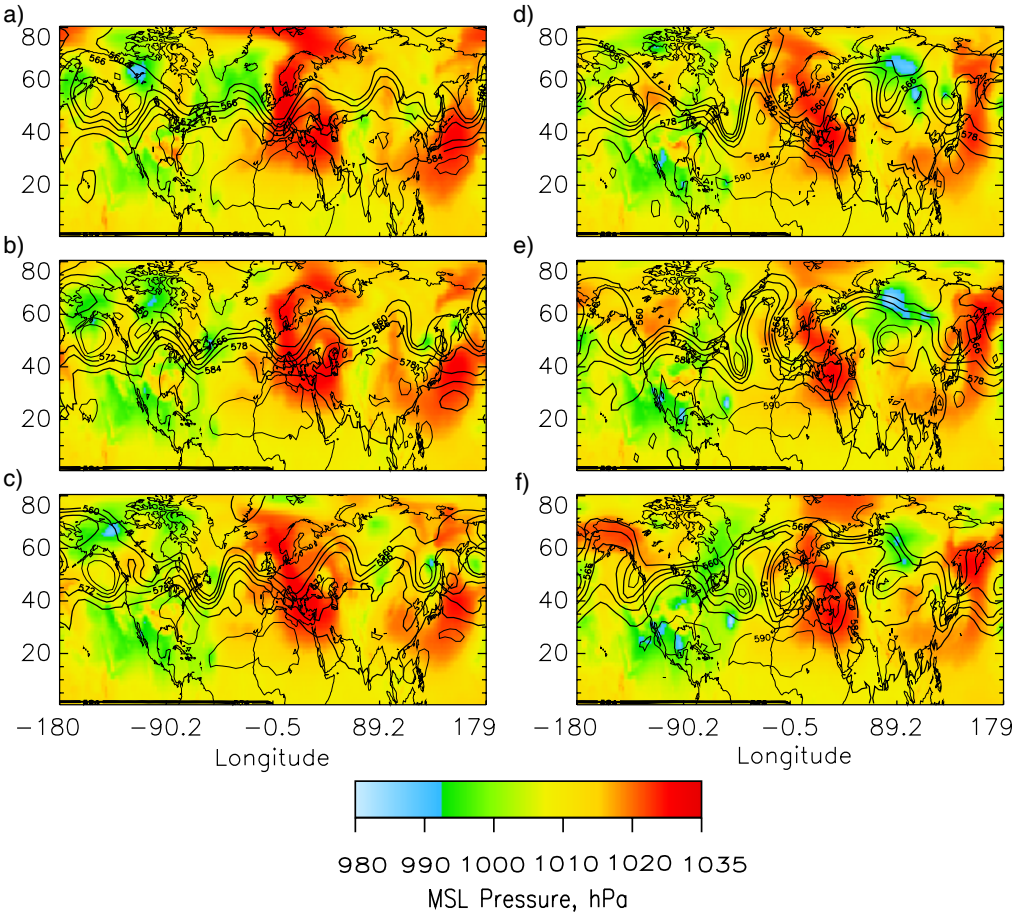

Fig. 5. Mean sea level pressure (MSL, hPa) at 12:00 UT for **(a)** 23 June 1997, **(b)** 24 June, **(c)** 25 June, **(d)** 26 June, **(e)** 27 June, and **(f)** 28 June. Contours depict the height of the 500 hPa surface in decameters.

In addition, the influence of each source region is extended by the transport winds and other meteorological conditions (for example, clouds responsible for aqueous conversion of SO_2 to sulfate) experienced during the simulation time period. For sulfate, the large (>50%) fractional contribution from NA sources was located in a geographically concentrated area (Fig. 3a), whereas large fractional contributions from Eu and As sources extended over much greater areas (Figs. 3b–c). It is especially notable that the large influence of As sources extended over the north Pacific to Alaska, western and northern Canada, and the west coast of the U.S. (Fig. 3c). The fractional contribution from biogenic (Bio) sources was small (between 10 and 20%) except for very limited areas with small sulfate burden and small contributions from other sources (Fig. 3d). The areas of large fractional contribution from volcanic (Vol) sources were southwest of Popocatépetl volcano and west of Kilauea volcano, Hawaii (Fig. 3e). Although SO_2 emissions from Etna volcano were ∼40% of those from Popocatépetl, the fractional contribution of sulfate from Etna is limited to ∼25% by the large contribution to sulfate column burden from Eu sources.

Sulfate distributions were relatively delocalized from source areas because it is a secondary species with a moderately long turnover time. In contrast, SO_2 was much more localized over source areas (Fig. 4) because it is a primary emitted species with a very short turnover time. As with sulfate, the areas of large (>50%) fractional contribution from NA sources to the SO_2 burden (Fig. 4a) were more limited than those of Eu and As sources (Figs. 4b–c). The areas of large fractional contribution from As sources extended into the eastern Pacific Ocean (Fig. 4c), but the value of the average SO_2 burden in this region was very small ($\sim 3\,\mu\mathrm{mol\,m^{-2}}$). Large fractional contributions from Bio sources were found in areas not influenced by large anthropogenic sources where the burdens were small, and in areas of large biogenic productivity (Fig. 4d). The areas of large fractional contribution from Vol sources were directly downwind of the more active volcanos, such as Popocatépetl (Mexico), Kilauea (Hawaii), Etna (Italy), and volcanos in Japan, Indonesia, and the Kamchatka peninsula (Fig. 4e). The "contrail"-like features over the oceans, such as the one extending from northeast to southwest across the middle of

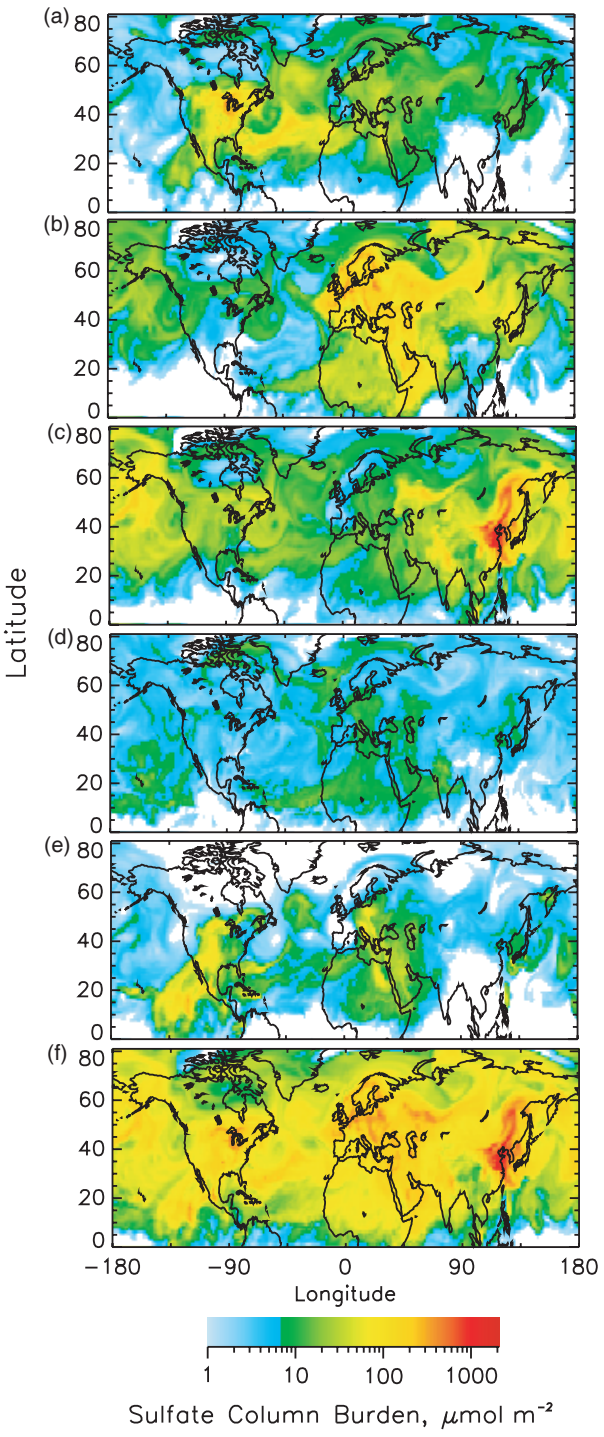

Fig. 6. Modeled sulfate column burdens for 29 June 1997 12:00 UT from **(a)** anthropogenic sources in North America, **(b)** anthropogenic sources in Europe, **(c)** anthropogenic sources in Asia, **(d)** biogenic sources, **(e)** volcanic sources, and **(f)** all sources. White denotes areas where the sulfate column burden was less that $1\,\mu\mathrm{mol\,m^{-2}}$.

the Atlantic Ocean (especially noticeable in Fig. 4a), are due to emissions from air and ship traffic in these corridors (Fig. 2a). These features are not evident in the sulfate distributions.

3 Meteorological influences

Here the influence of transport meteorology on the fractional contribution to the column burdens from emissions in the several source regions is examined via the mean sea level pressure, MSL, for 23 June to 28 June 1997 (Fig. 5); conditions on these days were representative of the entire simulation period. On 29 June column burdens of SO_2 and sulfate (Fig. 6) were affected by four major features of the global sea level pressure: large high pressure systems off the coast of Japan and over Europe, a low pressure system over northern Mexico and the eastern Pacific Ocean, and a strong low pressure system over Siberia. Transport of Asian emissions from sources located between 20° N and 40° N (Fig. 2a) to the north along the eastern coast of Asia and then eastward over the northern Pacific Ocean is evident in Fig. 6c. This transport was driven by clockwise flow around the high pressure system off the coast of Japan from 23 June to 25 June (Figs. 5a–c). After 25 June this high pressure system migrated northward, and a low pressure system developed in conjunction with an upper level cutoff low over Siberia and Eastern Asia (Fig. 5d). The low pressure system further enhanced northward transport of sulfate from emissions in southeast Asia; this was followed by flow around the high pressure system, which then transported the sulfate eastward across the Pacific at higher latitudes. From 23 June through 27 June (Figs. 5a–e) a large high pressure system over western Europe generated light winds and little vertical mixing, preventing transport of European emissions and enhancing production of sulfate. On 25 and 26 June (Figs. 5c–d) there was a decrease in surface pressure in phase with a deepening ridge-trough system at upper levels over Spain and north of the Indian sub-continent; counterclockwise flow around these systems transported sulfate from European sources northward (by the system over Spain) to Scandinavia and southward (by the system over India) to the Middle East. The low pressure that formed over Siberia on 25 June (Fig. 5c) enabled the eastward transport of sulfate from European sources to western and central Asia.

For several days preceding 28 June the North American continent was dominated by a deepening low pressure system over the southwestern U.S. and northern Mexico consistent with divergence at the 500 hPa level (Figs. 5a–e). A surface high pressure system was located over the southeastern U.S. through 27 June; on 28 June (Fig. 5f) there were low pressure systems over the Midwest U.S. and over the Gulf of Mexico. Counterclockwise flow associated with these systems transported emissions from the major east coast sources over the Atlantic Ocean (Fig. 6a). A deepening trough and associated

surface low pressure center in the Atlantic Ocean (Fig. 5f) kept the maximum sulfate column burden south of 35° N until the eastern side of the pressure center (∼45° W) was reached, when emissions were transported towards the north Atlantic. These meteorological patterns assist in explaining features seen in the average fractional contribution to the sulfate and SO_2 burden (Figs. 3 and 4) such as the abrupt decrease in the contribution of NA sources at the west coast of the continent, the large influence of As sources over the western and northern Pacific Ocean, and of Eu sources over the Middle East, extending to central Asia and the Atlantic Ocean south of 20° N and north of 60° N for sulfate.

In the interactive discussion of this paper one of the anonymous reviewers suggested that links between meteorology and concentration or burden might be strengthened, perhaps by the use of trajectory analysis. As noted in the introduction several investigators have in fact used trajectory calculations to attribute modeled species to source regions, at least qualitatively. Here, rather than using trajectory analysis we have taken the approach of attributing sulfate (and SO_2) to large source regions by labeling the sulfur species according to several source regions. We take this approach for several reasons: First, the labeling approach readily yields quantitative estimates of contributions to concentration from the several source regions; second, as the source regions considered here are continental in scale, they are not well suited to examination by trajectory analysis; third, the accuracy of trajectories decreases markedly after ∼5 days; fourth, the use of different assumptions and methodologies in trajectory calculations can yield quite different results; and finally, trajectory-based approaches cannot accurately represent nonlinear chemical reactions, such as the H_2O_2-SO_2 reaction, which is dominant in sulfate formation. As an alternative means of relating atmospheric burdens of sulfate and SO_2 to emissions regions, we would invite the reader to examine the animations of the column burdens of these substances taken from the model output at 6-h intervals, available at http://www.ecd.bnl.gov/steve/model/junejuly97.html, which are an effective way to follow the transport of these substances.

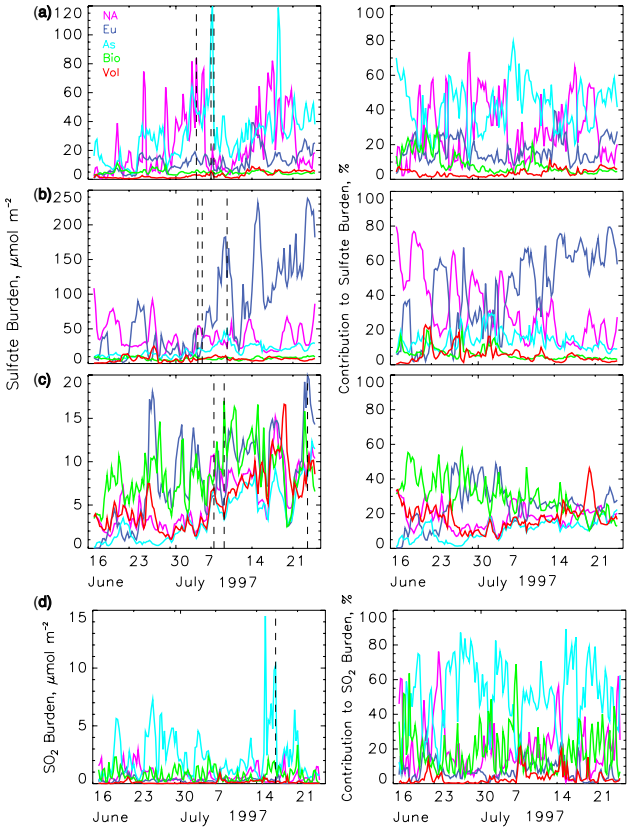

Fig. 7. Time series of the sulfate column burden attributable to the different source regions and source types in magnitude (left) and as fraction of total (right) at several locations shown in Fig. 2. **(a)** model grid cell that includes Seattle, WA, USA (122° W, 47° N), **(b)** model grid cell that includes Sagres, Portugal (8° W, 36° N), and **(c)** model grid cell that includes Barbados (59° W, 13° N). Panel **(d)** shows similar time series for the SO_2 column burden at a model grid cell in the mid north Pacific Ocean (170° W, 47° N).

4 Attribution by source regions

Three locations in areas in which there were substantial contributions to sulfate mixing ratios and burdens from two or more source regions or source types (Fig. 2b) were selected to illustrate the temporal variability and the vertical structure of these contributions: the model grid cells that include Seattle, WA, USA (122.20° W, 47.36° N, grid cell surface height 0.1 km), Sagres, Portugal (8.95° W, 36.98° N, grid cell surface height <0.01 km), and Barbados (59.43° W, 13.17° N, grid cell surface height <0.01 km). Time series of the sulfate column burden for these three locations (Figs. 7a–c) exhibit substantial variation in the absolute and relative contributions from the different source regions. At Seattle the apportionment of the column burden for the entire modeling period was As sources 42%, NA sources 32%, and Eu sources 16%. Despite the long transit across the north Pacific As sources were the principal contributors on two of the three instances of largest magnitude of the total column burden (Fig. 7a). At Sagres the apportionment was Eu sources 52%, NA sources 26%, and As sources 13%. The situation at Barbados (Fig. 7c) was much more complicated; the apportionment here was Bio sources 27%, Eu sources 26%, NA sources 17%, and Vol sources 17%. At different time periods each of the different source regions and source types (except As sources) was the major contributor to the column burden. Sulfate from NA sources reaching Barbados was transported east across the North Atlantic, south along the west coasts of Europe and Africa and west to Barbados via the trade winds at lower latitudes. Sulfate from Eu sources reaching Barbados was transported south

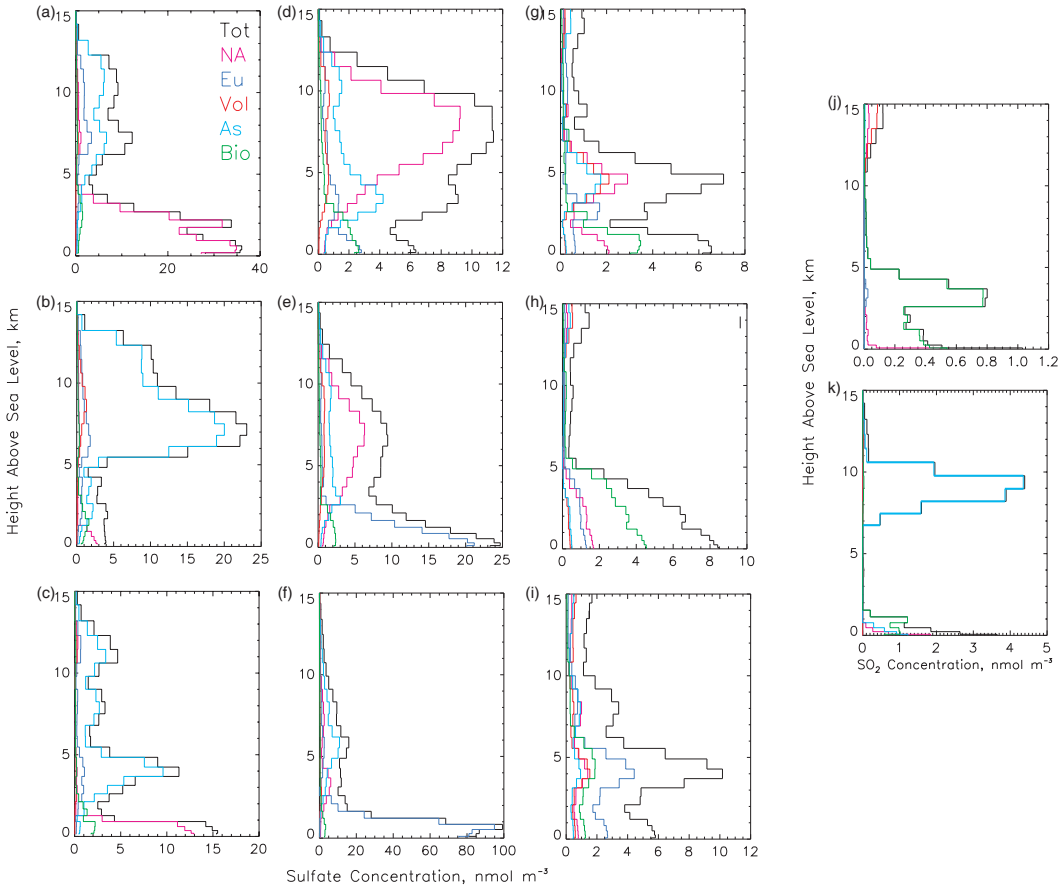

Fig. 8. Vertical profiles of the sulfate concentration attributable to the different source regions and source types at several locations shown in Fig. 7. Model grid cell that includes Seattle, WA, USA (122° W, 47° N) on **(a)** 4 July 1997 12:00 UT, **(b)** 7 July 00:00 UT, and **(c)** 7 July 12:00 UT; model grid cell that includes Sagres, Portugal (8° W, 36° N) on **(d)** 4 July 18:00 UT, **(e)** 5 July 12:00 UT, and **(f)** 9 July 18:00 UT; model grid cell that includes Barbados (59° W, 13° N) on **(g)** 7 July 12:00 UT, **(h)** 9 July 06:00 UT, and **(i)** 23 July 12:00 UT. Vertical profiles of the SO_2 concentration attributable to the different source regions and source types at **(j)** Barbados on 9 July 06:00 UT, and **(k)** a model grid cell in the mid north Pacific Ocean (170° W, 47° N) on 17 July 06:00 UT. Note the individual scale for the concentration axis on each panel.

along western Europe and Africa and west to Barbados via the trade winds. Sulfate from As sources reaching Barbados was transported east across the North Pacific, across North America, and then followed the same path as sulfate from NA sources. Animations of the sulfate and SO_2 column burdens from each source region are available at URL http://www.ecd.bnl.gov/steve/model/junejuly97.html.

Vertical profiles of the sulfate concentration for these locations at selected times (Fig. 8) show marked differences in the distribution with height of the contribution attributable to the different source regions and types. At Seattle on 4 July 1997 (Fig. 8a) the maximum concentration was near the surface and NA sources dominated below 3 km; above 6 km the principal contributors were As sources, with a smaller but perceptible contribution from Eu sources. Sulfate from Eu sources reaching Seattle is transported east across Europe, Asia, and the North Pacific Ocean. A very different picture is presented on 7 July, at 00:00 UT. On this date the largest concentration was substantially displaced from the surface (∼7 km) and quite isolated from low altitude processes; the principal contributors above 5 km were As sources; below this height several source regions and source types contributed almost equally to a much smaller concentration. Just 12 h later (Fig. 8c) the picture was again quite different, with considerably lower concentrations overall. The maximum concentration was in a shallow layer below 1 km, contributed mostly by NA sources, but there was still substantial material from As sources aloft, and these sources continued to dominate the column burden. The influence of As sources at Seattle for these three dates is demonstrated using the sulfate column burden (Figs. 9a–c). On 4 July at 12:00 UT the Asian plume entered the Seattle area from the southwest (Fig. 9a); the full effect of this plume was felt on 7 July at 00:00 UT (Fig. 9b), and by 7 July at 12:00 UT the plume had passed to the east of Seattle (Fig. 9c).

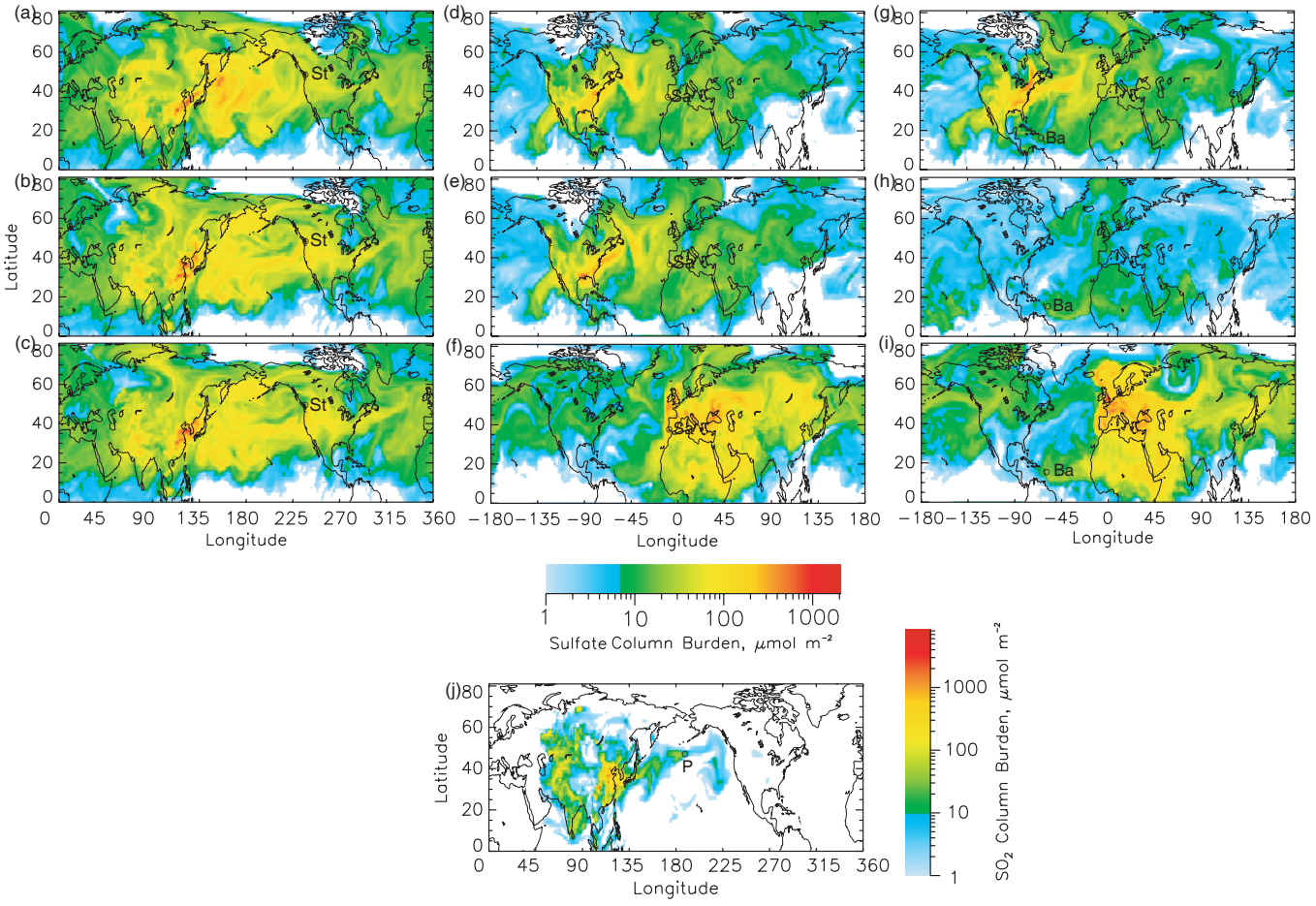

Fig. 9. Sulfate column burden from **(a)** Asian sources on 4 July 1997 12:00 UT, **(b)** Asian sources on 7 July 00:00 UT, **(c)** Asian sources on 7 July 12:00 UT, **(d)** North American sources on 4 July 18:00 UT, **(e)** North American sources on 5 July 12:00 UT, **(f)** European sources on 9 July 18:00 UT, **(g)** North American sources on 7 July 12:00 UT, **(h)** biogenic sources on 9 July 06:00 UT, and **(i)** European sources on 23 July 12:00 UT. SO_2 column burden from **(j)** Asian sources on 17 July 06:00 UT. St= Seattle, Sa= Sagres, Ba= Barbados, P= mid north Pacific Ocean location. White denotes areas where the column burden from individual source was less that 1 μmol m^{-2}.

At Sagres the maximum sulfate concentrations varied by almost a factor of eight ($\sim$13 to 100 nmol m^{-3}) for the dates presented here. On 4 July 1997 at 18:00 UT (Fig. 8d) the concentration was small; NA sources were the principal contributors in a fairly deep layer between 6 and 8 km where the largest concentration ($\sim$13 nmol m^{-3}) was located. On 5 July at 12:00 UT (Fig. 8e) the principal contributors below 2.5 km were Eu sources and the largest concentration was at the surface ($\sim$25 nmol m^{-3}); in addition there was a plume between 3 and 12 km where the principal contributors were NA sources. On 9 July at 18:00 UT (Fig. 8f) the principal contributors below 3 km were Eu sources and the largest concentration was also at the surface ($\sim$100 nmol m^{-3}); the principal contributors above 4 km were As sources, and the concentration ($\sim$15 nmol m^{-3}) was similar to that on 4 July at 18:00 UT. The animation of the sulfate column burden from As sources showed that the contribution from these sources was transported in a wave pattern across the Pacific Ocean at $\sim$40° N latitude, across North America at $\sim$45° N, across the Atlantic Ocean at $\sim$50° N and finally southward over Sagres. The influence of NA and Eu sources on Sagres is shown in Figs. 9d–e. On 4 July 1997 at 18:00 UT (Fig. 9d) the plume from NA sources had reached Sagres from the west via a wave pattern across the Atlantic Ocean (see animation). By 5 July at 12:00 UT the column burden from these sources had started to decrease (Fig. 9e), and on 9 July at 18:00 UT (Fig. 9f) the large column burden from Eu sources had advanced over Sagres from the east (see animation).

Barbados presented a more complicated picture because several source regions and source types were the main contributors or contributed about equally to the sulfate concentration at different times. On the three dates shown the sulfate concentration was similar ($\sim$10 nmol m^{-3}) but up to a factor of five to ten less than at Seattle and Sagres, mainly a consequence of this location being well removed from major emission sources. An example of a very mixed picture is that

for 7 July (Fig. 8g). On this date sulfate was present mostly in two distinct layers, one below 2 km to which Bio sources contributed slightly over half and to which NA sources contributed ∼30% of the concentration, and a second layer, between 4 and 6 km, to which NA, Vol, and As sources contributed almost equally. On 9 July (Fig. 8h) most of the material was in a deep layer extending from the surface to ∼6 km, to which Bio sources from the Atlantic ocean south of 25° N (Fig. 2b) were the largest contributors below 6 km; however, about half of the concentration in this altitude range was contributed by other source regions and types. On 23 July at 12:00 UT (Fig. 8i) three somewhat distinct layers were evident; from the surface to ∼2 km and also from 2 km to 4 km Eu sources contributed ∼40% of the concentration, with all other source regions and source types contributing about equally to the remaining 60%. All source types contributed about equally to the third layer, centered at ∼8 km. The influence of NA, Bio, and Eu sources on Barbados is seen also in the sulfate column burden (Figs. 9g–i).

In contrast to the distribution of sulfate, time series of the SO_2 column burden at the selected locations showed that the major contributors were always proximate sources: North American sources at Seattle (∼96%), European sources at Sagres (∼94%), and biogenic sources at Barbados (∼64%). However, at Barbados some vertical structure was apparent during certain time periods, for example on 9 July 06:00 UT (Fig. 8j) Bio and NA sources contributed almost equally at the surface, but the NA contribution dropped rapidly with height whereas at the altitude of the maximum total concentration, ∼3 km, the SO_2 was contributed by Bio sources.

The influence of Asian sources on the SO_2 burden over the mid north Pacific Ocean was examined at 170° W, 47° N (Fig. 2b). At this location (∼4300 km from Tokyo; ∼5700 km from Beijing, major source regions on the Asian continent) As sources were responsible for more than half of the SO_2 burden for the entire simulation period. Time series of the SO_2 column burden at this location (Fig. 7d) showed that As sources were frequently the dominant contributors. The distribution of the SO_2 column burden from these sources during one of the time periods of large influence (17 July 06:00 UT, Fig. 9j) showed a narrow plume that meandered across the north Pacific Ocean. The vertical profile of the SO_2 concentration (Fig. 8k) at the mid ocean location showed that almost all the SO_2 from these sources was quite elevated, in a layer at altitudes of between ∼7 and 11 km. At such altitudes SO_2 is immune to removal by one of its major sinks, dry deposition and can thus persist for considerable time. Compact aerosol layers have been observed to travel great distances in the upper troposphere (Damoah et al., 2004; Jaffe et al., 2004; Ansmann et al., 2002; Wandinger et al., 2002; Forster et al., 2001).

Because of the short time period examined in the present study it is not known how representative the instances chosen for detailed examination, Seattle, Sagres, and Barbados are of the northwestern North American coastal region, the coastal European, and the trade winds of the North Atlantic, respectively. Clearly the temporal variability of the controlling meteorology plays a large role in the absolute and relative contributions of distant and proximate sources to the sulfate burden at a given location and time. Nonetheless the cases examined here show that distant sources can make a substantial contribution to the column burden of sulfate at the locations under examination.

5 Attribution of sulfate burden by formation process

Sulfur dioxide is converted to sulfate in the model by two different processes: gas-phase oxidation by OH in clear (cloud-free) air and aqueous-phase oxidation by H_2O_2 and O_3 in cloud water. As the model associates the sulfate formed by different processes with different sulfate variables, it is possible to examine the amount of sulfate present at a given time and location that has been formed by one or the other process. For the entire simulation period ∼62% of the sulfate present in the model domain was formed by aqueous-phase oxidation and ∼36% by gas-phase oxidation; ∼2% was primary sulfate. However the fractional contributions by the two oxidation mechanisms varied considerably as a function of location and, at a given location, as a function of time during the model run. For example, more than half the sulfate present in geographic regions with sparse cloudiness and precipitation, such as North Africa and the Middle East, and in regions with sources at high altitude, such as Mexico, was formed by gas-phase oxidation. The spatial and temporal variation in formation mechanism is due mainly to differences in meteorological conditions, most importantly the presence and liquid water content of clouds. While it must be recognized that the sulfate present at a specific time and location is a mix of material formed locally and material transported to that location, nonetheless examination of formation mechanism of the sulfate present at specific locations and times allows inferences to be drawn about the reasons for the differences.

Two contrasting locations (Fig. 2b) were chosen to study the time variation of the sulfate formation processes. At a semi-desert area of Algeria (5° E, 22° N, grid cell surface height 1.1 km) ∼58% of the sulfate present over the entire simulation period was formed via gas-phase oxidation, and gas-phase oxidation was the principal contributor to the burden at this location at all times during the model period except for a few days around 30 June, Fig. 10a. The animation of the SO_2 burden reveals that periods of larger contribution from gas-phase oxidation occurred when large amounts of SO_2 from the European continent were transported over the arid areas of North Africa, with the oxidation taking place over the Sahara region of Africa where the prevailing meteorological conditions (strong solar radiation, abundant OH, and low cloud water content) favor conversion to sulfate via this mechanism. On days with little transport of SO_2 from Europe, such as 27 to 30 June, the sulfate present at the

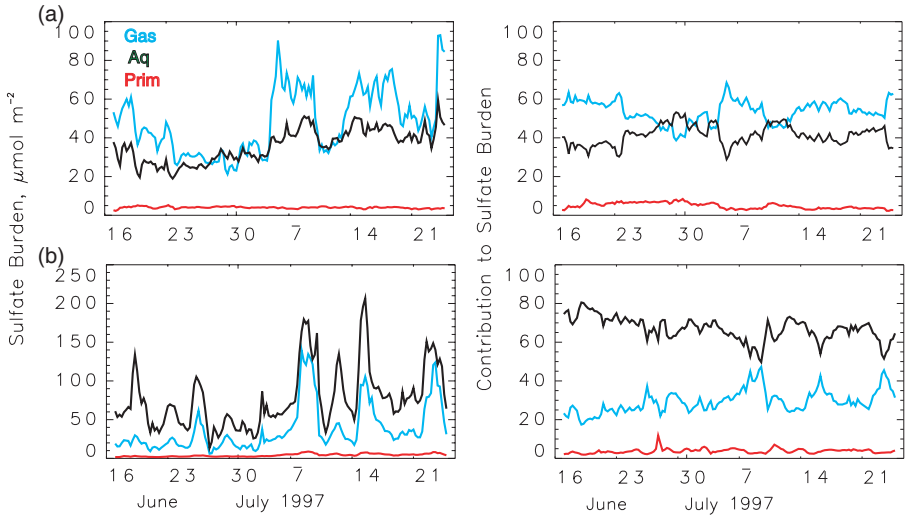

Fig. 10. Time series of the sulfate burden at **(a)** Algeria (5° E, 22° N), and **(b)** a location in the North Atlantic off the coast of Portugal (12° W, 39° N).

North African location was formed en route (over the European continent and the Mediterranean Sea), where conditions favored formation via aqueous-phase oxidation.

A contrasting situation is found over the western North Atlantic Ocean (Fig. 2b). Here, in order to permit comparison with measurements, we examined the model results in the study area of the ACE-2 cloudy Lagrangian-2 experiments, which were conducted 16 July to 18 July off the west coast of Portugal and Africa (11° to 15° W, 32° to 40° N, surface height 0) (Johnson et al., 2000a, b). At this location the dominant formation mechanism throughout the entire simulation period was aqueous-phase oxidation (Fig. 10b). The main features of the modeled vertical profile of the sulfate concentration (Fig. 11) at the approximate time and location of aircraft measurements during this study are consistent with the measured profiles of accumulation mode aerosol concentration reported in Fig. 7 of Johnson et al. and with the measured concentration of total condensation nuclei in Fig. 7 of Osborne et al. (2000) which show these quantities exhibiting a maximum below 1 km and decreasing with increasing altitude above. In addition, the larger contribution below 3 km of sulfate formed by aqueous-phase conversion supports the conclusions of Dore et al. (2000) that increases in the total aerosol mass at these altitudes observed during their experiment represented the net contribution to aerosol via conversion from gaseous precursors and that this conversion most probably occurred via in-cloud aqueous-phase reaction.

Summarizing Sects. 4 and 5, the time series of the sulfate column burden by source region and source type at specific locations for the entire simulation period and vertical profiles of the sulfate concentration for specific times and locations demonstrate the large temporal variability, the frequently large fractional contribution by remote sources, and

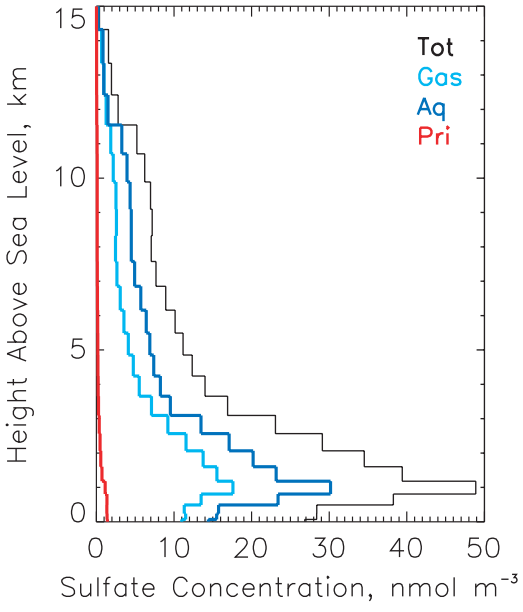

Fig. 11. Vertical profile of the sulfate concentration at 12° W, 39° N on 16 July 1997 at 00:00 UT.

the frequent occurrence of maximum concentrations well aloft. Not infrequently, important contributions to the concentration from remote sources were located in elevated layers; thus these source regions contribute more to column properties such as optical depth than to surface air quality. At Barbados, well removed from major sources and influenced by several source regions and source types, even surface concentrations were substantially impacted by remote sources. The relative contributions of the gas-phase and the

aqueous-phase oxidation pathways to the sulfate column burden at particular locations were influenced by meteorological conditions encountered during transport.

The most important factors affecting the distribution of both sulfate and SO_2 were the locations of emissions sources and predominant meteorological conditions. Because of its longer turnover time of ∼7 days (Benkovitz et al., 2004), sulfate was transported further from the source regions than was SO_2 (turnover time ∼1 day), with conversion taking place concurrent with transport. Emitted species were generally transported from west to east, but substantial northward transport was identified for emissions from Asian sources and additional northward and southward transport was identified for emissions from European sources. In addition, intercontinental transport of aerosols, already identified in specific instances by measurements (Jaffe et al., 2003; Perry et al., 1999; Prospero, 1999; Wotawa and Trainer, 2000) and satellite observations (Husar et al., 2001), has been illustrated in the present modeling results.

6 Summary and implications

Results from an Eulerian chemical transport model have been analyzed to attribute sulfate and SO_2 concentrations and column burdens to specific source regions, source types and sulfate formation processes. Because of the relatively short turnover times of these species proximate anthropogenic sources were the principal contributors to the burdens in the several regions, but the influence of North American sources was dominant over almost all of the North Atlantic Ocean, and likewise the influence of Asian sources was dominant over almost all of the North Pacific Ocean. At a given location not infrequently distant source regions contributed widely differing fractional amounts of sulfate, especially when the peak of the vertical distribution of concentration was highly elevated. At Seattle, WA, U.S. Asian sources contributed 42% and European sources contributed 16% of the column burden for the simulation period as a whole; the largest contribution from Asian and European sources occurred in layers above ∼3 km. At Sagres, Portugal, North American sources contributed 26% and Asian sources contributed 13% of the column burden; when the total column burden was small North American sources were the largest contributor, mainly in layers 5 km above the surface. Smaller contributions from Asian sources were occasionally seen as layers at altitudes above ∼4 km; these layers had been transported eastward across the Pacific Ocean, North America, and the Atlantic Ocean.

Overall, the average contribution to the sulfate burden for the entire simulation period was 62% from aqueous-phase oxidation, 36% from gas-phase oxidation and 2% was primary sulfate; however, in areas of low cloudiness, such as north Africa and the Middle East, or areas at high altitudes, such as parts of Mexico, the fraction of sulfate formed by gas-phase oxidation was considerably enhanced, over 50%. At locations of low cloudiness where gas-phase oxidation was the main contributor to the sulfate concentration for certain time periods aqueous-phase oxidation was the main contributor in layers above the surface, as a consequence of long-range transport from cloudy areas.

It should be emphasized that the objective of the present study was to examine the extent to which distant sources contribute to the absolute and relative column burden of sulfate at specific locations at specific times, and the variability of these contributions during the time period examined, rather than to develop a statistically or climatologically robust attribution. Here we relied on a set of model runs that had been rigorously evaluated by comparison with observations at specific locations and for short time periods, typically, for sulfate, 24 h, but was, perforce, limited to a rather short model run, six weeks of a single year. While this rather short time period necessarily limits any generalization of the findings, the present findings nonetheless demonstrate instances in which the sulfate column burden at a given location was dominated by material that was transported across major oceanic basins and also demonstrate the high temporal variability of the relative and absolute contributions of this distant sulfate to the column burden at a given location.

In summary the present study contributes to a growing body of evidence indicative of the importance of long range transport of submicrometer aerosols on scales of several thousand kilometers. This contribution is especially important in a relative sense in regions of low background aerosol, such as over the North Pacific and North Atlantic where it might be expected to contribute strongly to aerosol indirect forcing in view of the low natural aerosol loading, which leads to high sensitivity to incremental aerosol loading (Schwartz et al., 2002). Such loadings can also be substantial in an absolute sense. For example in the calculations presented here for Seattle, the contribution of Asian sources to sulfate column burden was commonly 20 μmol m^{-2} and occasionally greater than 100 μmol m^{-2} (2–10 mg m^{-2}); for a mass scattering efficiency of 5–8 m^2 g^{-1} (Charlson et al., 1992) this burden would result in an optical depth of 0.01 to 0.08. In turn, for an aerosol radiative forcing efficiency of -40 to -50 W m^{-2} per optical depth (24-h; top of atmosphere; Anderson et al., 2005) this aerosol optical depth would result in a direct radiative forcing of 0.4 to 4 W m^{-2}. In contrast, because the long-range-transported aerosol was generally well elevated above the surface, it would appear that this aerosol makes a relatively small contribution to surface concentrations pertinent to air quality considerations.

Table A1. Schematic of the different species defined as variables in the model. Superscripts: a=aqueous-phase oxidation, g=gas-phase oxidation, p=primary emission. Subscripts: As=Asia, B=biogenic, Eu=European, Ext=external (coming from outside the model domain), NA=North American, Vol=volcanic.

Species 6	SO_2		Sulfate			DMS	MSA
Source 9	Primary	Gas-phase oxidation	Primary	Gas-phase oxidation	Aqueous-phase oxidation	Primary	Gas-phase oxidation
NA Anthropogenic (140° W to 30° W)	${}^{p}_{\mathrm{NA}}SO_2$		${}^{p}_{\mathrm{NA}}SO_4^{2-}$	${}^{g}_{\mathrm{NA}}SO_4^{2-}$	${}^{a}_{\mathrm{NA}}SO_4^{2-}$		
Eu Anthropogenic (30° W to 60° E)	${}^{p}_{\mathrm{Eu}}SO_2$		${}^{p}_{\mathrm{Eu}}SO_4^{2-}$	${}^{g}_{\mathrm{Eu}}SO_4^{2-}$	${}^{a}_{\mathrm{Eu}}SO_4^{2-}$		
Asia Anthropogenic (60° E to 140° W)	${}^{p}_{\mathrm{As}}SO_2$		${}^{p}_{\mathrm{As}}SO_4^{2-}$	${}^{g}_{\mathrm{As}}SO_4^{2-}$	${}^{a}_{\mathrm{As}}SO_4^{2-}$		
Volcanic	${}^{p}_{\mathrm{Vol}}SO_2$			${}^{g}_{\mathrm{Vol}}SO_4^{2-}$	${}^{a}_{\mathrm{Vol}}SO_4^{2-}$		
Biogenic		${}^{g}_{B}SO_2$		${}^{g}_{B}SO_4^{2-}$	${}^{a}_{B}SO_4^{2-}$	${}^{p}_{B}DMS$	${}^{g}_{B}MSA$
External		${}^{g}_{\mathrm{Ext}}SO_2$	${}^{p}_{\mathrm{Ext}}SO_4^{2-}$	${}^{g}_{\mathrm{Ext}}SO_4^{2-}$	${}^{a}_{\mathrm{Ext}}SO_4^{2-}$	${}^{p}_{\mathrm{Ext}}DMS$	

Appendix A

Description of the Eulerian model

The Eulerian model used in this work was developed from the model described in (Benkovitz et al., 1994). The model represents emissions of sulfur dioxide (SO_2) and dimethyl sulfide (DMS), transport, convective mixing, generation of hydrogen peroxide (H_2O_2) from the hydroperoxy radical (HO_2) in the gas-phase, chemical conversion of SO_2 to sulfate by H_2O_2 and ozone (O_3) in the aqueous-phase and by the hydroxyl radical (OH) in the gas-phase, chemical conversion of DMS to SO_2 and MSA by OH, wet removal, and dry deposition (Fig. 1). A hemispheric domain was used in this study because it incorporates all industrialized areas of the Northern Hemisphere, allows studies of the relative influences of the various source regions and source types and minimizes import/export of material into/out of the model domain. Because the chemistry of sulfur species alters atmospheric concentrations of oxidant species, the influence of source regions and source types was obtained by defining a different variable for each source region/type (Table A1) and performing only a single simulation; this method provides accurate estimates of such influences. The model was initialized with the mixing ratio of all species set to zero; material transported into the model domain was assigned representative background concentrations and was carried as a separate variable.

The meteorological data used to drive the model, for the modeling period 1 June–31 July 1997, were obtained from the European Centre for Medium-Range Weather Forecasts (ECMWF) (European Centre for Medium-Range Weather Forecasts, 2003). Mixing ratios (MRs) of oxidant species were based on monthly average MRs for June and July calculated using Version 2 of the Model of Ozone and Related Chemical Tracers, (MOZART) (Brasseur et al., 1998; Horowitz et al., 2003) driven by a GCM, the NCAR Community Climate Model. Anthropogenic emissions of SO_2 were based on the Emission Database for Global Atmospheric Research (EDGAR) Version 3.2 (Olivier et al., 2002) inventory, which represents annual emissions ca. year 1995. Seasonal emissions and the breakdown between release points below and above 100 m were calculated using the appropriate fractions from the Global Emissions Inventory Activity (GEIA) Version 1B inventory (Benkovitz et al., 1996); emissions for the Northern Hemisphere summer were used. Emissions of primary sulfate for 1997 were estimated from the GEIA SO_2 inventory as 1% of the sulfur emissions (by mole) for industrialized regions (North America, Europe) and 2% for the rest of the model domain. Sea surface DMS concentrations for June and July from Kettle et al. (1999) were combined with seawater DMS measurements made during the Aerosol Characterization Experiment-2 (ACE-2) field campaign (Raes and Bates, 1995) to calculate time- and location-dependent oceanic DMS emissions using the

wind speed transfer velocity relationship of Liss and Merlivat (1986). Seasonal emissions of DMS and hydrogen sulfide (H_2S) from land sources were calculated using the methodology of Lamb (Bates et al., 1992) gridded to $1^\circ \times 1^\circ$ resolution (Benkovitz et al., 1994); these emissions were treated entirely as DMS in the model. Volcanic emissions are quite variable temporally and there were substantial volcanic events during the modeling period, so as far as possible daily sulfur emissions from volcanos were specific to the simulation period and were treated entirely as SO_2. The principal sources of time-specific information were the Volcano Activity Reports compiled by the Global Volcanism Program of the Smithsonian Institution available at web site http://www.volcano.si.edu/reports/bulletin/index.cfm (accessed in spring 1999) and personal communications from investigators conducting measurements at individual volcanos.

Acknowledgements. Research was performed under the auspices of the U.S. Department of Energy under Contract No. DE-AC02-98CH10886 and was supported in part by the NOAA Office of Global Programs. The meteorological data used to drive the model were obtained from the European Centre for Medium-Range Weather Forecasts (ECMWF), Reading, UK.

Edited by: F. J. Dentener

References

Allan, J. D., Bower, K. N., Coe, H., Boudries, H., Jayne, J. T., Canagaratna, M. R., Millet, D. B., Goldstein, A. H., Quinn, P. K., Weber, R. J., and Worsnop, D. R.: Submicron aerosol composition at Trinidad Head, California, during ITCT 2K2: Its relationship with gas phase volatile organic carbon and assessment of instrument performance, J. Geophys. Res.-Atmos., 109(D23), D23S24, doi:10.1029/2003JD004208, 2004.

Anderson, T. L., Charlson, R. J., Bellouin, N., Boucher, O., Chin, M., Christopher, S. A., Haywood, J., Kaufman, Y. J., Kinne, S., Ogren, J. A., Remer, L. A., Takemura, T., Tanré, D., Torres, O., Trepte, C. R., Wielicki, B. A., Winker, D. M., and Yu, H.: A-Train strategy for quantifying direct climate forcing by anthropogenic aerosols, Bull. Am. Meteorol. Soc., 86, 1795–1809, 2005.

Ansmann, A., Wandinger, U., Wiedensohler, A., and Leiterer, U.: Lindenberg Aerosol Characterization Experiment 1998 (LACE 98): Overview, J. Geophys. Res., 107(D21), 8129, doi:10.1029/2000JD000233, 2002.

Bates, T. S., Lamb, B. K., Guenther, A., Dignon, J., and Stoiber, R. E.: Sulfur Emissions to the Atmosphere from Natural Sources, J. Atmos. Chem., 14, 315–337, 1992.

Bellouin, N., Boucher, O., Haywood, J., and Reddy, M. S.: Global estimate of aerosol direct radiative forcing from satellite measurements, Nature, 438, 1138–1141, doi:10.1038/nature04348, 2005.

Benkovitz, C. M., Berkowitz, C. M., Easter, R. C., Nemesure, S., Wagener, R., and Schwartz, S. E.: Sulfate Over the North Atlantic and Adjacent Continental Regions: Evaluation for October and November, 1986 Using a Three-Dimensional Model Driven by Observation-Derived Meteorology, J. Geophys. Res., 99(D10), 20 725–20 756, 1994.

Benkovitz, C. M., Scholtz, M. T., Pacyna, J., Tarrasón, L., Dignon, J., Voldner, E. V., Spiro, P. A., Logan, J. A., and Graedel, T. E.: Global Gridded Inventories of Anthropogenic Emissions of Sulfur and Nitrogen, J. Geophys. Res., 101(D22), 29 239–29 253, 1996.

Benkovitz, C. M., Schwartz, S. E., and Kim, B.-G.: Evaluation of a Chemical Transport Model for Sulfate using ACE-2 Observations and Attribution of Sulfate Mixing Ratios to Source Regions and Formation Processes, Geophys. Res. Lett., 30(12), doi:10.1029/2003GL016942, 2003.

Benkovitz, C. M., Schwartz, S. E., Jensen, M. P., Miller, M. A., Easter, R. C., and Bates, T. S.: Modeling atmospheric sulfur over the Northern Hemisphere during the Aerosol Characterization Experiment 2 experimental period, J. Geophys. Res., 109, D22207, doi:10.1029/2004JD004939, 2004.

Bott, A.: A Positive Definite Advection Scheme Obtained by Nonlinear Renormalization of the Advective Fluxes, Mon. Wea. Rev., 117, 1006–1015, 1989.

Brasseur, G., Hauglustaine, D., Walters, S., Rasch, P., Müller, J., Granier, G., and Tie, X. X.: MOZART: A Global Chemical Transport Model for Ozone and Related Chemical Tracers. 1. Model Description, J. Geophys. Res., 103(D21), 28 265–28 289, 1998.

Charlson, R. J., Schwartz, S. E., Hales, J. M., Cess, R. D., Coakley Jr., J. A., Hansen, J. E., and Hofmann, D. J.: Climate forcing by anthropogenic aerosols, Science, 255, 423–430, 1992.

Damoah, R., Spichtinger, N., Forster, C., James, P., Mattis, I., Wandinger, U., Beirle, S., Wagner, T., and Stohl, A.: Around the World in 17 days – Hemispheric-Scale Transport of Forest Fire Smoke from Russia in May 2003, Atmos. Chem. Phys., 4, 1311–1321, 2004.

Dore, A. J., Johnson, D. W., Osborne, S. R., Choularton, T. W., Bower, K. N., Andreae, M. O., and Bandy, B. J.: Evolution of Boundary-Layer Aerosol Particles Due to In-Cloud Chemical Reactions During the 2nd Lagrangian Experiment of ACE-2, Tellus, 52B(2), 452–462, 2000.

Easter, R. C.: Two Modified Versions of Bott's Positive Definite Numerical Advection Scheme, Mon. Wea. Rev., 121, 297–304, 1993.

Easter, R. C. and Luecken, D. J.: A Simulation of Sulfur Wet Deposition and Its Dependence on the Inflow of Sulfur Species to Storms, Atmos. Environ., 22(12), 2715–2739, 1988.

European Centre for Medium-Range Weather Forecasts: IFS Documentation Cycle CY25r1 Parts I–VII, European Centre for Medium-Range Weather Forecasts, Reading, England, 2003.

Forster, C., Wandinger, U., Wotawa, G., James, P., Mattis, I., Althausen, D., Simmonds, P., O'Doherty, S., Jennings, S. G., Kleefeld, C., Schneider, J., Trickl, T., Kreipl, S., Jäger, H., and Stohl, A.: Transport of Boreal Forest Fire Emissions from Canada to Europe, J. Geophys. Res., 106(D19), 22 887–22 906, 2001.

Graf, H.-F., Feichter, J., and Langmann, B.: Volcanic Sulfur Emissions: Estimates of Source Strenght and Its Contribution to the Global Sulfate Distribution, J. Geophys. Res., 102(D9), 10 727–10 738, 1997.

Horowitz, L. W., Walters, S., Mauzerall, D., Emmons, L., Rasch, P., Granier, C., Tie, X., Lamarque, J. F., Schultz, M., and Brasseur,

G.: A global simulation of tropospheric ozone and related tracers: Description and evaluation of MOZART, version 2, J. Geophys. Res., 108(D24), 4784, doi:10.1029/2002JD002853, 2003.

Husar, R. B., Tratt, D. M., Schichtel, B. A., Falke, S. R., Li, F., Jaffe, D., Gassó, S., Gill, T., Laulainen, N. S., Lu, F., Reheis, M. C., Chun, Y., Westphal, D., Holben, B. N., Gueymard, C., McKendry, I., Kuring, N., Feldman, G. C., McClain, C., Frouin, R. J., Merrill, J., DuBois, D., Vignola, F., Murayama, T., Nickovic, S., Wilson, W. E., Sassen, K., Sugimoto, N., and Malm, W. C.: Asian dust events of April 1998, J. Geophys. Res., 106(D16), 18 317–18 330, doi:10.1029/2000JD900788, 2001.

Jaffe, D., Anderson, T., Covert, D., Kotchenruther, R., Trost, B., Danielson, J., Simpson, W., Berntsen, T., Karlsdottir, S., Blake, D., Harris, J., Carmichael, G., and Uno, I.: Transport of Asian Air Pollution to North America, Geophys. Res. Lett., 26(6), 711–714, 1999.

Jaffe, D., McKendry, I., Anderson, T., and Price, H.: Six 'New' Episodes of Trans-Pacific Transport of Air Pollutants, Atmos. Environ., 37, 391–404, 2003.

Jaffe, D., Bertschi, I., Jaeglé, L., Novelli, P., Reid, J. S., Tanimoto, H., Vingarzan, R., and Westphal, D. L.: Long-Range Transport of Siberian Biomass Burning Emissions and Impact on Surface Ozone in Western North America, Geophys. Res. Lett., 31, L16106, doi:10.1029/2004GL020093, 2004.

Johnson, D. W., Osborne, S., Wood, R., Suhre, K., Johnson, R., Businger, S., Quinn, P. K., Wiedensohler, A., Durkee, P. A., Russell, L. M., Andreae, M. O., O'Dowd, C., Noone, K. J., Bandy, B., Rudolph, J., and Rapsomanikis, S.: An Overview of the Lagrangian Experiments Undertaken During the North Atlantic Aeorosol Characterisation Experiment (ACE-2), Tellus, 52B(2), 290–320, 2000a.

Johnson, R., Businger, S., and Baerman, A.: Lagrangian Air Mass Tracking with Smart Balloons During ACE-2, Tellus, 52B(2), 321–334, 2000b.

Kettle, A. J., Andreae, M. O., Amoroux, D., Andreae, T. W., Bates, T. S., Berresheim, H., Bingemer, H., Boniforti, R., Curran, M. A. J., DiTullio, G. R., Helas, G., Jones, G. B., Keller, M. D., Kiene, R. P., Leck, C., Levasseur, M., Malin, G., Maspero, M., Matrai, P., McTaggart, A. R., Mihalopoulos, N., Nguyen, B. C., Nuovo, A., Putaud, J. P., Rapsomanikis, S., Roberts, G., Schbeske, G., Sharma, S., Simo, R., Staubes, R., Turner, S., and Uher, G.: A Global DataBase of Sea Surface Dimethyl Sulfide (DMS) Measurements and a Procedure to Predict Sea Surface DMS as a Function of Latitude, Longitude, and Month, Global Biogeochem. Cycles, 13, 399–444, 1999.

Liepert, B. G.: Observed Reductions of Surface Solar Radiation at Sites in the United States and Worldwide from 1961 to 1990, Geophys. Res. Lett., 29(10), 1421, doi:10.1029/2002GL014910, 2002.

Liss, P. S. and Merlivat, L.: Air-Sea Gas Exchange Rates: Introduction and Synthesis, in: The Rate of Air-Sea Exchange in Geochemical Cycling, edited by: Buat-Menard, P., D. Reidel Publishing Company, Dordrecht, p. 113–127, 1986.

Malcom, A. L., Derwent, R. G., and Maryon, R. H.: Modeling the Long-Range Transport of Secondary PM_{10} to the UK, Atmos. Environ., 34(6), 881–894, 2000.

Martin, B. D., Fuelberg, H. E., Blake, N. J., Crawford, J. H., Logan, J. A., Blake, D. R., and Sachse, G. W.: Long-Range Transport of Asian Overflow to the Equatorial Pacific, J. Geophys. Res., 108(D2), 8322, doi:10.1029/2001JD001418, 2003.

NASA: Chemical Kinetics and Photochemical Data for Use in Stratospheric Modeling. Evaluation #12., pp. 266, National Aeronautics and Space Administration, Jet Propulsion Laboratory, Pasadena, 1997.

Olivier, J. G. J., Peters, J. A. H. W., Bakker, J., Berdowski, J. J. M., Visschedijk, A. J. H., and Bloos, J. P. J.: Applications of EDGAR: Emissions Database for Global Atmospheric Research, pp. 151, National Institute for Public Health and the Environment (RIVM)/Netherlands Organization for Applied Scientific Research (TNO), Bilthoven, The Netherlands, 2002.

Osborne, S. R., Johnson, D. W., Wood, R., Bandy, B. A., Andreae, M. O., O'Dowd, C. D., Glantz, P., Noone, K. J., Gerbig, C., Rudolph, J., Bates, T. S., and Quinn, P.: Evolution of the Aerosol, Cloud and Boundary-Layer Dynamic and Thermodynamic Characteristics During the 2nd Lagrangian Experiment of ACE-2, Tellus, 52B(2), 375–400, 2000.

Penner, J., Andreae, M., Annegarn, H., Barrie, L., Feichter, J., Hegg, D., Jayraman, A., Leaitch, R., Murphy, D., Nganga, J., and Pitari, G.: Aerosols, their Direct and Indirect Effects, in: Climate Change 2001: The Scientific Basis, edited by: Houghton, J. T., Din, Y., Griggs, D. J., Noguer, M., v. d. Linden, P. J., Dai, X., Maskell, K., and Johnson, C. A., Cambridge University Press, Cambridge, UK, p. 289–348, 2001.

Perry, K. D., Cahill, T. A., Schnell, R. C., and Harris, J. M.: Long-Range Transport of Anthropogenic Aerosols to the National Oceanic and Atmospheric Administration Baseline Station at Mauna Loa Observatory, Hawaii, J. Geophys. Res., 104(D15), 18 521–18 535, 1999.

Pielke, R. A., Cotton, W. R., Walko, R. L., Tremback, C. J., Lyons, W. A., Grasso, L. D., Nicholls, M. E., Moran, M. D., Wesley, D. A., Lee, T. J., and Copeland, J. H.: A comprehensive meteorological modeling system – RAMS, Meteorol. Atmos. Phys., 49, 69–91, 1992.

Piketh, S. J., Swap, R. J., Maenhaut, W., Annegarn, H. J., and Formetti, P.: Chemical Evidence of Long-Range Atmospheric Transport over Southern Africa, J. Geophys. Res., 107(D24), 4817, doi:10.1029/2002JD-2056, 2002.

Prospero, J. M.: Long-Term Measurements of the Transport of African Mineral Dust to the Southeastern United States: Implications for Regional Air Quality, J. Geophys. Res., 104(D13), 15 917–15 927, 1999.

Raes, F. and Bates, T.: ACE-2 North Atlantic Regional Aerosol Characterization Experiement, Office for Official Publications of the European Communities, Brussels-Luxembourg, 1995.

Ramaswamy, V., Boucher, O., Haigh, J., Hauglustaine, D., Haywood, J., Myhre, G., Nakajima, T., Shi, G. Y., and Solomon, S.: Radiative Forcing of Climate Change, in: Climate Change 2001: The Scientific Basis, edited by: Houghton, J. T., Din, Y., Griggs, D. J., Noguer, M., v. d. Linden, P. J., Dai, X., Maskell, K., and Johnson, C. A., Cambridge University Press, Cambridge, UK, p. 349–416, 2001.

Rasch, P. J., Barth, M. C., Kiehl, J. T., Schwartz, S. E., and Benkovitz, C. M.: A Description of the Global Sulfur Cycle and Its Controlling Processes in NCAR CCM3., J. Geophys. Res., 105(D1), 1367–1385, 2000.

Schwartz, S. E.: Mass-Transport Limitation to the Rate of In-Cloud Oxidation of SO_2: Re-Examination in the Light of New Data, Atmos. Environ., 22(11), 2491–2499, 1988.

Schwartz, S. E., Harshvardhan, and Benkovitz, C. M.: Influence of anthropogenic aerosol on cloud optical depth and albedo shown by satellite measurements and chemical transport modeling, Proc. Natl. Acad. Sci. USA, 99, 1784–1789, 2002.

Sheih, C. M., Wesely, M. L., and Walcek, C. J.: A Dry Deposition Module for Regional Acid Deposition, U.S. Environmental Protection Agency, Research Triangle Park, NC, 1986.

Stanhill, G. and Cohen, S.: Global Dimming: a Review of the Evidence for a Widespread and Significant Reduction in Global Radiation with Discussion of its Probable Causes and Possible Agricultural Consequences, Agric. and Forest Met., 107, 255–278, 2001.

U.S. Environmental Protection Agency: National Air Quality and Emissions Trends Report, 1999, p. 237, U.S. Environmental Protection Agency, Office of Air Quality Planning and Standards, Research Triangle Park, NC, 2001.

Uno, I., Carmichael, G. R., Streets, D. G., Tang, Y., Yienger, J. J., Satake, S., Wang, Z., Woo, J.-H., Guttikunda, S., Uematsu, M., Matsumoto, K., Tanimoto, H., Yoshioka, K., and Iida, T.: Regional Chemical Weather Forecasting System CFORS: Model Descriptions and Analysis of Surface Observations at Japanese Island Statons During the ACE-Asia Experiment, J. Geophys. Res., 108(D23), 8668, doi:10.1029/2002JD002845, 2003.

Walcek, C. J. and Taylor, G. R.: A Theoretical Method for Computing Vertical Distributions of Acidity and Sulfate Production Within Cumulus Clouds, J. Atmos. Sci., 43, 339–355, 1986.

Wandinger, U., Müller, D., Böckmann, C., Althausen, D., Matthias, V., Bösenberg, J., Weiß, V., Fiebig, M., Wendisch, M., Stohl, A., and Ansmann, A.: Optical and Microphysical Characterization of Biomass-Burning and Industrial-Pollution Aerosols from Multiwavelength Lidar and Aircraft Measurements, J. Geophys. Res., 107(D21), 8125, doi:10.1029/2000JD000202, 2002.

Wesely, M.: Parameterization of Surface Resistances to Gaseous Dry Deposition in Regional-Scale Numerical Models, Atmos. Environ., 23, 1293–1304, 1989.

Wotawa, G. and Trainer, M.: The Influence of Canadian Forest Fires on Pollutant Concentrations in the United States, Science, 288, 324–328, 2000.

Yienger, J. J., Galanter, M., Holloway, T. A., Phadnis, M. J., Guttikunda, S. K., Carmichael, G. R., Moximm, W. M., and II, H. L.: The Episodic Nature of Air Pollution Transport from Asia to North America, J. Geophys. Res., 105(D22), 26 931–26 946, 2000.

Yin, F., Grosjean, D., Flagan, R. C., and Seinfeld, J. H.: Photooxidation of Dimethyl Sulfide and Dimethyl Disulfide. II: Mechanism Evaluation, J. Atmos. Chem., 11, 365–399, 1990a.

Yin, F., Grosjean, D., and Seinfeld, J. H.: Photooxidation of Dimethyl Sulfide and Dimethyl Disulfide. I: Mechanism Development, J. Atmos. Chem., 11, 309–364, 1990b.